Electron scattering from domain walls in ferromagnetic Luttinger liquids

N. Sedlmayr,[1,*] S. Eggert,[1,2] and J. Sirker[1,2]

[1]*Department of Physics, University of Kaiserslautern, D-67663 Kaiserslautern, Germany*

[2]*Research Center OPTIMAS, University of Kaiserslautern, D-67663 Kaiserslautern, Germany*

(Received 26 February 2011; revised manuscript received 17 May 2011; published 15 July 2011)

We study the properties of interacting electrons in a one-dimensional conduction band coupled to bulk noncollinear ferromagnetic order. The specific form of noncollinearity we consider is that of an extended domain wall. The presence of ferromagnetic order breaks spin-charge separation and the domain wall introduces a spin-dependent scatterer active over the length of the wall λ. Both forward and backward scattering off the domain wall can be relevant perturbations of the Luttinger liquid and we discuss the possible low-temperature phases. Our main finding is that backward scattering, while determining the ultimate low-temperature physics, only becomes important at temperatures $T/J < \exp(-\lambda/\lambda_+)$, with J being the magnetic exchange and λ_+ the backward scattering length scale. In physical realizations, $\lambda \gg \lambda_+$ and the physics will be dominated by forward scattering, which can lead to a charge-conducting but spin-insulating phase. In a perturbative regime at higher temperatures we furthermore calculate the spin and charge densities around the domain wall and quantitatively discuss the interaction-induced changes.

DOI: 10.1103/PhysRevB.84.024424 PACS number(s): 71.10.Pm, 73.21.Hb, 75.30.Hx, 71.15.−m

I. INTRODUCTION

In a one-dimensional electron system, particlelike excitations cannot survive in the presence of interactions leading to a breakdown of Fermi liquid theory. Instead, the excitations are of a collective, bosonic nature and can be described by a universal low-energy effective theory, the Luttinger liquid (LL).[1–3] Impurities are expected to play a particularly important role in one dimension, because electrons are not able to circumvent them. Studies have indeed revealed that impurities in many cases are relevant perturbations effectively cutting the chain and therefore impeding transport at low temperatures.[4–10] More surprisingly, however, there are also situations where the low-temperature behavior in the presence of multiple impurities corresponds to "healing," i.e., to perfect transmission.[5,6]

One of the hallmarks of the LL is spin-charge separation. This means that the normal modes of the Luttinger model have either spin or charge character and are completely decoupled. Spin-charge separation, however, only holds in the case of spin degeneracy. In the presence of a magnetic field—which leads to spin-split bands—the normal modes of the Luttinger model acquire a mixed character. This situation was first studied in Refs. 11 and 12 using the Hubbard model in a magnetic field as a starting point. One obvious question to ask is how impurities affect the low-temperature properties in such a system. Since spin and charge are no longer decoupled, we might expect new low-energy fixed points which are not covered by the standard Kane and Fisher picture.[5]

Of experimental relevance is, in particular, the case of electrons in a quasi-one-dimensional wire coupled to bulk ferromagnetic order. Domain walls in the ferromagnet then act as spatially extended magnetic impurities for the electrons in the wire. Such systems of coupled electronic and magnetic degrees of freedom have received considerable interest,[13] spurred, in particular, by possible applications as magnetic domain-wall racetrack memories.[14] However, the focus has principally been on how the transport properties of free electrons behave in a ferromagnetic wire with a domain wall and how these spin-polarized currents set the domain wall itself into motion. An interesting question to ask then is whether electron-electron interactions can become important in such cases. Aside from some work on mean-field[15] and Hartree-Fock[16,17] interactions, there is little consideration in the literature of how the electronic and magnetic behavior of quasi-one-dimensional ferromagnetic systems is modified in a strongly correlated system.

In particular, the case of a ferromagnetic LL with a domain wall present has not yet been fully addressed. In the limit of an infinitely sharp domain wall, Pereira and Miranda[18] have considered an effective low-temperature model containing only a spin-flip backscattering term. Based on this model, they have argued that the domain-wall scattering in the ultimate low-temperature limit is the magnetic analog of the Kane-Fisher problem.[5,6,11] In other words, at low temperatures either a spin-charge insulator or a LL is found. In addition to the spin-flip backscattering process considered in Ref. 18, however, also a pure potential (spin-independent) backscattering term is allowed by symmetry.[16,17] By starting from a model for an extended domain wall we show that such a term is indeed present and can be important for the physics at very low temperatures. Our main focus, however, is what happens in the more physically relevant regime of longer domain walls and higher temperatures. The behavior of the system in this case remains unknown, and it is that question we wish to address here.

There are three possible temperature regimes in this problem and it is convenient to introduce here some notation for them. At high temperatures we have a "perturbative regime," where the domain-wall scattering can be treated as a small perturbation. As we consider lower temperatures the perturbative treatment will break down due to the presence of relevant operators. At first we may still consider the domain wall as an extended region and we refer to this as the "extended regime." This regime is the focus of our study. At even lower temperatures in the renormalization group flow

the domain wall will become effectively δ-function-like and we can treat the relevant operators as boundary terms. This regime we refer to as the "sharp regime" and is the regime which has been previously discussed in the literature.[16–18] In the sharp regime, the spin-flip and the potential backscattering terms with scattering length λ_+ are the possible relevant perturbations determining the low-temperature physics. We show, however, that if we start from a system with an extended domain wall with length $\lambda \gg \lambda_+$, then temperatures $T/J < \exp(-\lambda/\lambda_+)$, with J being the magnetic exchange, are required to enter this regime. This regime, therefore, is only accessible if one already starts with a very sharp domain wall, a situation which can possibly be realized by nanoconstrictions.[19]

Experimentally, the construction of ferromagnetic chains of single magnetic atoms is already possible.[20] In such systems the ferromagnetic order is observed to extend over small distances separated by regions of noncollinearity.[20–24] It is important to note that these chains are assembled on some substrate and therefore cannot be considered as fully isolated one-dimensional systems. Therefore, the Mermin-Wagner theorem,[25] which forbids long-range ferromagnetic order at finite temperatures in a strictly one-dimensional system with sufficiently short-range interactions, does not apply. Furthermore, the substrate has consequences for the effective spin exchange between the atoms. The spin exchange tensor can quite generally be decomposed into a symmetric and an antisymmetric part. In spin chains which are part of a regular three-dimensional crystal the antisymmetric part is often forbidden by inversion symmetry. For chains of single magnetic atoms on a substrate, on the other hand, both terms are expected to be present so that noncollinear spin order is a generic property of such systems. The presence of the substrate might also disguise the LL properties of the atomic wire and our model system might therefore be too simplistic to directly apply to this situation. Nevertheless, it might serve as a starting point for the investigation of more realistic models.

Other possible candidates to which our model might apply include dilute magnetic semiconductors[26] and low-temperature ferromagnetic metals.[27,28] Systems where the magnetic and electronic degrees of freedom belong to different layers would also be a possible realization. Furthermore, we want to point out that our analysis is also valid for a quantum wire with a nonuniform external magnetic field applied.

Our paper is organized as follows. In Sec. II we introduce the model and derive the low-energy effective theory by linearizing the excitation spectrum followed by bosonization. In Sec. III we consider the first-order renormalization group (RG) equations for the various scattering processes and discuss the fixed points of the RG flow in the extended and sharp regimes. In Sec. IV we study an experimentally accessible temperature regime where the relevant scattering terms can be treated perturbatively. We discuss different cases depending on the hierarchy of the different length scales present in the problem and calculate the spin and charge densities around the domain wall. In the final section we present a brief summary of our results and some additional conclusions.

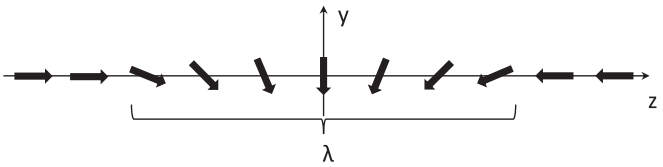

FIG. 1. A schematic view of the magnetization orientation in the wire. λ is the length of the domain wall.

II. THE MODEL

We will consider an "s-d"-like model in which the bulk magnetization and the conduction electrons are treated separately (though, of course, still coupled). We assume two time scales in the problem, a fast electronic one and a slow magnetic one. This allows us to answer the question of how the presence of the domain wall affects the LL, forgetting the effect the motion of the domain wall will have on the conduction electrons. For the already mentioned dilute magnetic semiconductors and, in particular, ferromagnetic metals this model with separate electronic and magnetic degrees of freedom, active on different time scales, is a realistic starting point.

The direction of the bulk magnetization of the wire can be described by a unit vector $\vec{n}(z) = \cos[\Theta(z)]\hat{\mathbf{z}} + \sin[\Theta(z)]\hat{\mathbf{y}}$ and we consider, in particular, the case $\cos[\Theta(z)] = -\tanh[z/\lambda]$ describing the spatial profile of a domain wall of length λ situated at $z = 0$; this is plotted schematically in Fig. 1. The magnetization is coupled to the conduction band electrons with a strength given by the exchange coupling J. We consider a screened, and hence short-range, interaction $V(z - z')$. To simplify the presentation we consider here a spin-independent, SU(2) symmetric interaction. We want to point out, however, that the low-energy theory [Eqs. (3) and (4)] obtained after linearizing the excitation spectrum remains valid for a spin-dependent interaction $V_{\sigma\sigma'}(z - z')$ as long as the interaction is spin conserving.

We start from the following standard s-d Hamiltonian,[29] $\tilde{H} = \tilde{H}_0 + \tilde{H}_M + H_I$:

$$\begin{aligned}
\tilde{H}_0 &= \int dz\, \tilde{\psi}^\dagger_\sigma(z)\Big[-\frac{1}{2m}\partial_z^2 - \mu\Big]\tilde{\psi}_\sigma(z),\\
\tilde{H}_M &= -\frac{J}{2}\int dz\, \tilde{\psi}^\dagger_\sigma(z)\tilde{\psi}_{\sigma'}(z)\vec{\sigma}_{\sigma\sigma'}\cdot\vec{n}(z), \qquad (1)\\
H_I &= \frac{1}{2}\int dz\, dz'\tilde{\psi}^\dagger_\sigma(z)\tilde{\psi}^\dagger_{\sigma'}(z')V(z-z')\tilde{\psi}_{\sigma'}(z')\tilde{\psi}_\sigma(z).
\end{aligned}$$

Here $\tilde{\psi}^\dagger_\sigma(z)$ is the creation operator for an electron of spin σ at a position z, μ is the chemical potential, m is the electron mass, and summation over the spin indices $\{\sigma,\sigma'\}$ is implied. Due to the incommensurate nature of the spin-split Fermi points we gain no advantage from explicitly considering half or full filling and the filling factor is left general. We do exclude, however, the case of very small filling where the Fermi energy ε_F would become so small that a linearization of the spectrum would only be appropriate at very low temperatures. Furthermore, we only want to consider the case where the filling in both bands is nonzero; i.e., we are not interested in the fully spin-polarized "half-metallic" case,[30] which would

bring us back to an effective spinless fermion model. In the following we set $\hbar = 1$ and $k_B = 1$.

In order to be able to linearize the system our first step must be to remove the spatially dependent, and in principle perhaps very large, magnetization. This is achievable by rotating the spin direction around the x axis to a collinear ferromagnetic alignment via the following gauge transformation:[31,32] $\mathbf{H} = \mathbf{U}^\dagger(z)\tilde{\mathbf{H}}\mathbf{U}(z)$, $\psi_\sigma(z) = U^\dagger_{\sigma\sigma'}(z)\tilde{\psi}_{\sigma'}(z)$, and $\mathbf{U}(z) = e^{\frac{i}{2}\Theta(z)\sigma^x}$. The interaction is left unaffected as it is SU(2) invariant, the magnetization is locally rotated to a Zeeman term $\tilde{H}_M \to H_M$, and a gauge potential is introduced: $\tilde{H}_0 \to H_0 + H_G$. Thus, $H = H_0 + H_G + H_I + H_M$ and

$$\begin{aligned} H_0 &= \sum_\sigma \int dz\, \psi^\dagger_\sigma(z)\left[-\frac{1}{2m}\partial_z^2 - \mu\right]\psi_\sigma(z), \\ H_G &= \frac{1}{8m}\sum_{\sigma\sigma'}\int dz \psi^\dagger_\sigma(z)[\Theta'(z)]^2\delta_{\sigma\sigma'}\psi_{\sigma'}(z) \\ &\quad -\frac{1}{4m}\sum_{\sigma\sigma'}\int dz[\psi^\dagger_\sigma(z) i\Theta'(z)\sigma^x_{\sigma\sigma'}\partial_z\psi_{\sigma'}(z) \\ &\quad -(\partial_z\psi^\dagger_\sigma(z)) i\Theta'(z)\sigma^x_{\sigma\sigma'}\psi_{\sigma'}(z)], \\ H_M &= -\frac{J}{2}\sum_\sigma\int dz\, \psi^\dagger_\sigma(z)\sigma^z_{\sigma\sigma}\psi_\sigma(z), \end{aligned} \tag{2}$$

with $\Theta'(z) = [\lambda\cosh(z/\lambda)]^{-1}$. The gauge potential has been written in a manifestly Hermitian form. The first term of H_G is a pure potential scatterer, the next two terms describe spin-flip scattering. Without H_G this is simply a spin-split band model[11] (see Fig. 2). In our model the gauge potential introduces extended scattering terms, active over the length of the domain wall, which have to be included and are important for the low-energy physics. The amplitudes of the spin-flip scattering and the potential term are proportional to λ/λ_F and $(\lambda/\lambda_F)^2$, respectively, where λ_F is the Fermi wavelength. We are here mainly interested in the case $\lambda \gg \lambda_F$. Except for very low temperatures the potential scattering term can then be safely neglected. On the other hand, in the limit of a sharp domain wall $\lambda \to 0$, then $\Theta'(z) \to \pi\delta(z)$, the scattering terms become boundary operators, and both the spin-flip and the potential scatterer have to be taken into account. We discuss these issues in greater depth in Sec. III.

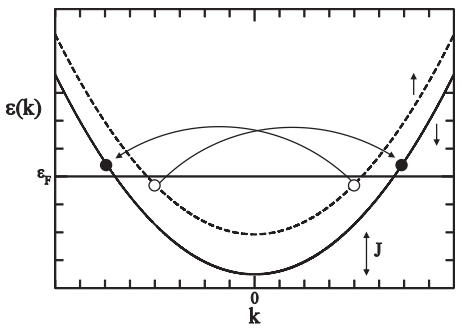

FIG. 2. A schematic view of the spin-split bands. One of the $g_{1\perp}$ processes is shown, which involve spin-flip scattering between left- and right-moving electrons.

The Hamiltonian (2) is now amenable to the usual bosonization procedure,[3] the first step of which is linearization via the ansatz $\psi_\sigma(z) = e^{ik_{F\sigma}z}\psi_{\sigma+}(z) + e^{-ik_{F\sigma}z}\psi_{\sigma-}(z)$, where $k_{F\sigma} = \sqrt{2m(\mu \pm J/2)}$. The $+$ and $-$ indices denote the right- and left-moving electrons, respectively. Note that if the Zeeman term is large we *must* linearize around the spin-split Fermi points, leading to the breakdown of spin-charge separation. After linearization we have $H_0 + H_M \to H_{0\uparrow} + H_{0\downarrow}$, with the linearized Hamiltonians

$$H_{0\sigma} = v_{F\sigma}\int dz[\psi^\dagger_{\sigma-}(z) i\partial_z\psi_{\sigma-}(z) - \psi^\dagger_{\sigma+}(z) i\partial_z\psi_{\sigma+}(z)], \tag{3}$$

where $m v_{F\sigma} = k_{F\sigma}$.

The interaction H_I can be decomposed into spin-parallel and spin-perpendicular components and written as

$$\begin{aligned} \tilde{H}_2 &= \sum_{\sigma,r=\pm}\int dz\left[\frac{\tilde{g}_{2\parallel\sigma}}{2}\rho_{\sigma r}\rho_{\sigma -r} + \frac{g_{2\perp}}{2}\rho_{\sigma r}\rho_{\bar{\sigma} -r}\right], \\ H_4 &= \sum_{\sigma,r=\pm}\int dz\left[\frac{g_{4\parallel\sigma}}{2}\rho_{\sigma r}\rho_{\sigma r} + \frac{g_{4\perp}}{2}\rho_{\sigma r}\rho_{\bar{\sigma} r}\right], \quad \text{and} \\ H_1 &= \sum_{\sigma,r=\pm}\int dz\Bigg[-\frac{g_{1\parallel\sigma}}{2}\rho_{\sigma r}\rho_{\sigma -r} \\ &\quad + \frac{g_{1\perp\sigma}}{2}e^{2iz(k_{F\bar{\sigma}} - k_{F\sigma})}\psi^\dagger_{\sigma r}\psi^\dagger_{\bar{\sigma} -r}\psi_{\bar{\sigma} r}\psi_{\sigma -r}\Bigg]. \end{aligned} \tag{4}$$

Here we have suppressed the spatial indices and defined the local density $\rho_{\sigma\pm} = \psi^\dagger_{\sigma\pm}\psi_{\sigma\pm}$. Note that the "$g$-ology" given here refers to the already rotated model, not the original physical picture. The chiral electrons of this linearized model, physically speaking, have a noncollinear spin orientation throughout the wire. Umklapp processes scattering two left movers into right movers and vice versa are always neglected here due to the noncommensurate nature of the Fermi wave vectors. We can rescale the $g_{2\parallel\sigma}$ term to include the $g_{1\parallel\sigma}$ process by redefining $g_{2\parallel\sigma} = \tilde{g}_{2\parallel\sigma} - g_{1\parallel\sigma}$ with $\tilde{H}_2 \to H_2$. The final $g_{1\perp\sigma}$ process, schematically shown in Fig. 2, cannot be formulated as a density-density interaction.

Finally, we have our model to be bosonized. We introduce the chiral bosonic fields $\phi_{\sigma r}(z)$.[3] The vertex operator is

$$\psi_{\sigma r}(z) = \frac{1}{\sqrt{2\pi\alpha}}e^{ir\sqrt{2\pi}\phi_{\sigma r}(z)}, \tag{5}$$

where α is a short distance cutoff. This leads to the following expression for the densities:

$$\rho_{\sigma r}(z) = -\frac{1}{\sqrt{2\pi}}\partial_z\phi_{\sigma r}. \tag{6}$$

Thus, we can write the quadratic part of the bosonic Hamiltonian, H_q, which is composed from H_0, H_M, H_2, H_4 as a matrix equation,

$$H_q = \int dz[\partial_z\Phi(z)]^T\mathbf{M}\partial_z\Phi(z); \tag{7}$$

$[\Phi(z)]^T = (\phi_{\uparrow+}, \phi_{\uparrow-}, \phi_{\downarrow+}, \phi_{\downarrow-})$. The bosonization procedure is thus sufficient to reexpress all but $H_{1\perp}$ and H_G in terms of a diagonalizable quadratic bosonic Hamiltonian. The matrix,

M, is

$$\mathbf{M} = \frac{1}{8\pi}\begin{pmatrix} 4\pi v_{F\uparrow} + 2g_{4\parallel\uparrow} & g_{2\parallel\uparrow} & g_{4\perp} & g_{2\perp} \\ g_{2\parallel\uparrow} & 4\pi v_{F\uparrow} + 2g_{4\parallel\uparrow} & g_{2\perp} & g_{4\perp} \\ g_{4\perp} & g_{2\perp} & 4\pi v_{F\downarrow} + 2g_{4\parallel\downarrow} & g_{2\parallel\downarrow} \\ g_{2\perp} & g_{4\perp} & g_{2\parallel\downarrow} & 4\pi v_{F\downarrow} + 2g_{4\parallel\downarrow} \end{pmatrix}.$$

M is a real symmetric matrix and, as such, has real eigenvalues. We can now diagonalize **M** and we do so in several steps to fully show the comparison with more standard expressions. In order for our final normal modes to have positive velocities there is a condition on this diagonalization procedure, given in the Appendix. However, for any realistic microscopic model this condition should always be met, which can be shown explicitly in the case of the Hubbard model in a magnetic field.[11]

We can now make two unitary transformations. The first is $\phi_{\sigma\pm} = (\phi_\sigma \mp \theta_\sigma)/\sqrt{2}$. Note that θ_σ is the adjoint of ϕ_σ and they satisfy $[\phi_\sigma(z), \Pi_\sigma(z')] = i\delta(z - z')$, where $\Pi_\sigma(z) = \partial_z\theta_\sigma(z)$. This first rotation has the effect of uncoupling the two adjoint fields. The second transformation is to rotate to the spin-charge representation: $\phi_{c/s}(z) = [\phi_\uparrow(z) \pm \phi_\downarrow(z)]/\sqrt{2}$ [and similar for the $\theta(z)$ fields]. The effect of these two rotations can be summarized as $\tilde{\mathbf{M}} = \tilde{\mathcal{U}}^{-1}\mathcal{U}^{-1}\mathbf{M}\mathcal{U}\tilde{\mathcal{U}}$, with $[\tilde{\Phi}(z)]^T = [\Phi(z)]^T\mathcal{U}\tilde{\mathcal{U}}$ [see Eqs. (A3) and (A4) in the Appendix]. If $[\tilde{\Phi}(z)]^T = (\phi_s, \phi_c, \theta_s, \theta_c)$, then our rotated Hamiltonian is defined by the matrix

$$\tilde{\mathbf{M}} = \frac{1}{2}\begin{pmatrix} \frac{v_s}{K_s} & v_b & 0 & 0 \\ v_b & \frac{v_c}{K_c} & 0 & 0 \\ 0 & 0 & v_s K_s & v_a \\ 0 & 0 & v_a & v_c K_c \end{pmatrix}. \tag{8}$$

Here K_s and K_c are the spin and charge Luttinger parameters, v_s and v_c are the spin and charge velocities, and v_a and v_b describe the coupling between the spin and charge sectors. These parameters are functions of the interaction strengths and Fermi velocities and to lowest order can be calculated directly [see Eq. (A1) in the Appendix]. At the noninteracting SU(2) symmetric point $K_s = K_c = 1$. In the case of spin degeneracy we find, as expected, $v_a = v_b = 0$ and the spin and charge modes decouple.

The nonquadratic contributions from H_G in this representation are

$$H^f_{Gsf} = \frac{g_f}{2\pi m\alpha}\int dz\Theta'(z)\sin[\sqrt{2\pi}\theta_s(z)] \times \sin[z(k_{F\uparrow} - k_{F\downarrow}) + \sqrt{2\pi}\phi_s(z)],$$

$$H^b_{Gsf} = \frac{g_b}{2\pi m\alpha}\int dz\Theta'(z)\sin[\sqrt{2\pi}\theta_s(z)] \times \sin[-z(k_{F\uparrow} + k_{F\downarrow}) + \sqrt{2\pi}\phi_c(z)],$$

$$H^f_{Gp} = -\frac{1}{8m}\sqrt{\frac{2}{\pi}}\int dz[\Theta'(z)]^2\partial_z\phi_c(z), \quad \text{and}$$

$$H^b_{Gp} = -\frac{1}{8\pi m}\sum_\sigma\int dz g_{b\sigma}[\Theta'(z)]^2 \times \cos[2zk_{F\sigma} + 2\sqrt{\pi}\phi_\sigma(z)]. \tag{9}$$

The first term, H^f_{Gsf}, describes a forward-scattering (upper index "f") spin-flip (lower index "sf") process where a fermion is exchanged between the spin up and spin down bands but stays on the same side of the Fermi surface. The second term, H^b_{Gsf}, is a backward-scattering spin-flip term where a fermion is exchanged between the bands and also moves from one side of the Fermi surface to the other. The third contribution H^f_{Gp} is a potential (lower index "p") spin-conserving forward-scattering process. The final term, H^b_{Gp}, is a spin-conserving backward-scattering process. This is the scatterer considered by Kane and Fisher which gives rise to the usual insulating fixed point.[5] All scattering processes are only active over the length of the domain wall (or, more generally speaking, the region of noncollinear spin order), where $\Theta'(z) \neq 0$. The scattering coupling constants for forward and backward spin-flip scattering from the domain wall are given by $g_{f/b} = k_{F\uparrow} \pm k_{F\downarrow}$. We have also introduced the bare potential scattering values $g_{b\sigma} = 1/\alpha$ for convenience.

The nonquadratic interaction term $H_{1\perp}$ is then

$$H_{1\perp} = \frac{2}{(2\pi\alpha)^2}\int dz\cos\left[2\sqrt{2\pi}\phi_s(z)\right] \times \left[g_{1\perp\uparrow}e^{-2iz(k_{F\uparrow}-k_{F\downarrow})} + g_{1\perp\downarrow}e^{2iz(k_{F\uparrow}-k_{F\downarrow})}\right]. \tag{10}$$

This last term also corresponds to a backward-scattering process. It stems, however, from the interaction H_I and therefore involves two fermions being scattered between the different bands and from one side of the Fermi surface to the other. These contributions have their simplest interpretation in terms of the spin and charge modes. However, the spin and charge modes are not eigenmodes of the model, see Eq. (8), and we also require Eqs. (9) and (10) in the appropriately rotated basis.

The diagonalization of $\tilde{\mathbf{M}}$ introduces new velocities, u_i, for H_q and a set of $\{T_i^{\theta,\phi}\}$ parameters. It can be summarized as

$$\begin{pmatrix}\phi_c(z)\\ \phi_s(z)\end{pmatrix} = \begin{pmatrix}\tilde{T}_1^\phi & \tilde{T}_2^\phi \\ T_1^\phi & T_2^\phi\end{pmatrix} \times \begin{pmatrix}\phi_1(z)\\ \phi_2(z)\end{pmatrix} \quad \text{and}$$
$$\begin{pmatrix}\theta_c(z)\\ \theta_s(z)\end{pmatrix} = \begin{pmatrix}\tilde{T}_1^\theta & \tilde{T}_2^\theta \\ T_1^\theta & T_2^\theta\end{pmatrix} \times \begin{pmatrix}\theta_1(z)\\ \theta_2(z)\end{pmatrix}, \tag{11}$$

with the parameters $\{T_i^{\theta,\phi}\}$ as given in Eq. (A6) of the Appendix. They are all known in terms of the previously mentioned Luttinger parameters. We have also simultaneously rescaled the fields to obtain two distinct eigenvalues rather than four. The final Hamiltonian is $H = H_q + H_{1\perp} + H^f_{Gsf} + H^b_{Gsf} + H^b_{Gp} + H^f_{Gp}$, where

$$H_q = \frac{u_i}{2}\int dz\,[(\partial_z\phi_i(z))^2 + (\Pi_i(z))^2] \tag{12}$$

and, with summation over i and j implied,

$$\begin{aligned}
H^f_{Gsf} &= \frac{g_f}{2\pi m\alpha}\int dz\,\Theta'(z)\sin\left[\sqrt{2\pi}T_i^\theta\theta_i(z)\right]\\
&\quad\times\sin\left[z(k_{F\uparrow}-k_{F\downarrow}) + \sqrt{2\pi}T_j^\phi\phi_j(z)\right],\\
H^b_{Gsf} &= \frac{g_b}{2\pi m\alpha}\int dz\,\Theta'(z)\sin\left[\sqrt{2\pi}T_i^\theta\theta_i(z)\right]\\
&\quad\times\sin\left[-z(k_{F\uparrow}+k_{F\downarrow}) + \sqrt{2\pi}\tilde{T}_j^\phi\phi_j(z)\right],\\
H^f_{Gp} &= -\frac{1}{8m}\sqrt{\frac{2}{\pi}}\int dz[\Theta'(z)]^2\tilde{T}_i^\phi\partial_z\phi_i(z), \quad \text{and}\\
H^b_{Gp} &= -\frac{1}{8\pi m}\sum_\sigma\int dz g_{b\sigma}[\Theta'(z)]^2\\
&\quad\times\cos\left[2zk_{F\sigma} + \sqrt{2\pi}\left(\tilde{T}_i^\phi + \sigma^z_{\sigma\sigma}T_i^\phi\right)\phi_i(z)\right]
\end{aligned} \tag{13}$$

for the scattering terms and, finally,

$$\begin{aligned}
H_{1\perp} &= \frac{2}{(2\pi\alpha)^2}\int dz\cos\left[2\sqrt{2\pi}T_i^\phi\phi_i(z)\right]\\
&\quad\times\left[g_{1\perp\uparrow}e^{-2iz(k_{F\uparrow}-k_{F\downarrow})} + g_{1\perp\downarrow}e^{2iz(k_{F\uparrow}-k_{F\downarrow})}\right].
\end{aligned}$$

The appropriate excitations of such an SU(2) *asymmetric* model have no obvious physical interpretation. This effective bosonic field theory lays the foundation of our further analysis. A similar model is found by Braunecker *et al.*[33,34] in a different situation, and, of course, by Pereira and Miranda[18] but without the H^f_{Gsf} and $H_{1\perp}$ terms which do not play any role for very sharp domain walls where the length scale λ is no longer present. However, they also neglect H^b_{Gp}, which does play a role in the sharp wall limit. Indeed, it is this term which, when dominant, leads to the Kane and Fisher insulating fixed point. This will become clear in Sec. III where the case of a sharp domain wall is obtained as a specific limit in our general analysis.

III. LOW-ENERGY PHYSICS

In the generic case, we have three natural length scales present in the problem: $\lambda_+ \sim (k_{F\uparrow}+k_{F\downarrow})^{-1}$ related to spin-flip backward scattering, $\lambda_- \sim (k_{F\uparrow}-k_{F\downarrow})^{-1}$ related to spin-flip forward scattering, and the domain-wall length λ. In the limit of weak magnetization $\lambda_- \to \infty$ and $2\lambda_+ \to \lambda_F$ while, on the other hand, the limit of large magnetization, when one spin channel becomes frozen out, gives $\lambda_+ \approx \lambda_- \approx \lambda_F$. It is crucial for the further analysis to observe that the relative importance of the forward and backward-scattering terms is now not only determined by their scaling dimensions but also by the hierarchy of the three different length scales. Furthermore, in the RG flow we must distinguish between the extended and sharp regimes. In the beginning of the RG flow we have an extended domain wall and the scattering terms can be treated as bulk terms of dimension $d = 2$. However, when the ultraviolet momentum cutoff Λ during the RG process becomes of the order $1/\lambda$, then the extended domain wall will begin to look effectively pointlike, i.e., of dimension $d = 1$. The scattering terms then become boundary operators. At this stage the direction and rate of the flow of all of the operators can change, leading to the final low-temperature fixed points. For this effective $d = 1$ flow we must take the result of the $d = 2$ flow as the "zeroth-order" coupling constants. In physical terms, the domain wall starts to look pointlike if the electrons are correlated spatially over lengths much larger than the domain-wall length, i.e., if $J/T \gg \lambda/\alpha$.

Another important point to note is that for an extended domain wall we usually have $\lambda \gg \lambda_+$; i.e., the backward-scattering terms are strongly oscillating over the length of the domain wall. This leads to very small bare effective backward-scattering couplings which can be estimated as follows: The derivative of the domain-wall profile, $\Theta'(z)$, can be Fourier transformed leading to $\Theta'(k) = \pi/\cosh(\pi k\lambda/2)$. The nonoscillating component of the backward-scattering amplitude is then proportional to $g_b\Theta'(k = \pm 1/\lambda_+)$. Since $\Theta'(k)$ is a function which is sharply peaked at $k = 0$ for long domain walls, we have $|g_b\Theta'(k = \pm 1/\lambda_+)| \sim |g_b\exp(-\lambda/\lambda_+)| \ll 1$. If backward scattering is relevant, then the effective coupling constant will grow under the RG flow as

$$g_b^{\text{eff}} \sim g_b\exp(-\lambda/\lambda_+)\left(\frac{T_0}{T}\right)^{d-\gamma_b}, \tag{14}$$

where T_0 is an energy scale of order J. Backward scattering will only have an appreciable effect if the initially small bare coupling has again become of order 1 under the RG flow. This requires temperatures $T/J < \exp(-\lambda/\lambda_+)$ which are extremely small for many realistic situations. We therefore expect that forward scattering—ignored in previous investigations of the domain-wall problem—will play the dominant role in these cases.

Before discussing the various regimes any further, we want to derive the first-order RG equations for the forward- and backward-scattering terms. We start by writing a functional integral partition function[35]

$$\mathcal{Z} = \int D\phi_i D\Pi_i e^{-\int_0^\beta d\tau[\int dz[-i\Pi_i(z)\partial_\tau\phi_i(z)] + H[\Pi_i(z),\phi_i(z)]]}, \tag{15}$$

with periodic boundary conditions in imaginary time τ. Following the standard procedure we split the fields into fast, $\phi^>$, and slow, $\phi^<$, fields. Our fast fields are defined for $\Lambda' < |k|, |\omega|/u_i < \Lambda$, and the slow for $|k|, |\omega|/u_i < \Lambda'$, with Λ an ultraviolet cutoff. Expanding the exponent in terms of $H_{1\perp}$, $H^{f,b}_{Gsf}$, and H^b_{Gp} and performing the averaging over the fast modes we then reexponentiate the expression to find the appropriate scaling equations. The flow is parametrized in terms of l, defined as $\Lambda = \Lambda_0 e^{-l}$ and $\Lambda' = \Lambda_0 e^{-l-\delta l}$.

We find for the $H_{1\perp}$ term to first order that

$$\frac{dg_{1\perp\sigma}}{dl} = g_{1\perp\sigma}\Big[2 - \underbrace{2\left[\left(T_1^\phi\right)^2 + \left(T_2^\phi\right)^2\right]}_{\equiv\gamma_1}\Big]. \tag{16}$$

This term is an irrelevant perturbation ($\gamma_1 > 2$) for any realistic situation we are here interested in. In the limit of weak magnetization we can simplify the expression to find $\gamma_1 = 2K_s$. In this limit $K_s > 1$ and it becomes clear that the term is irrelevant.

The same analysis is performed on the domain-wall scattering terms. For spin-flip back scattering we find

$$\frac{dg_b}{dl} = g_b\Big[d - \underbrace{\tfrac{1}{2}\big[(\tilde{T}_1^{\phi})^2 + (\tilde{T}_2^{\phi})^2 + (T_1^{\theta})^2 + (T_2^{\theta})^2\big]}_{\equiv\gamma_b}\Big]. \quad (17)$$

As already mentioned d is the dimension of the wall, for spatially extended walls this is 2, whereas it is 1 in the limit of an infinitely sharp wall. As usual, the perturbation is relevant (irrelevant) if $\gamma_b < d$ ($\gamma_b > d$). In the limit of $J \to 0$ we can simplify this expression to $\gamma_b = [(K_s)^{-1} + K_c]/2$, consistent with Refs. 18 and 36. If we consider the Luttinger parameters for the Hubbard model in the zero magnetization limit we see that this term is always relevant for repulsive interactions both for $d = 1$ and $d = 2$ but can also become irrelevant in both cases for attractive interactions. In the general case described by Eq. (17) the relevance or irrelevance of backward scattering depends on the set of rotation parameters $T_i^{\theta,\phi}$ and no general conclusions are possible.

Similarly, the spin-flip forward-scattering equation stands as

$$\frac{dg_f}{dl} = g_f\Big[d - \underbrace{\tfrac{1}{2}\big[(T_1^{\phi})^2 + (T_2^{\phi})^2 + (T_1^{\theta})^2 + (T_2^{\theta})^2\big]}_{\equiv\gamma_f}\Big]. \quad (18)$$

In the limit of $J \to 0$ this simplifies to $\gamma_f = [(K_s)^{-1} + K_s]/2$. Since $K_s \geqslant 1$, in this limit it follows that $\gamma_f \geqslant 1$. For the case of a sharp wall ($d = 1$) forward scattering is therefore always irrelevant.[18,36] In the case of an extended wall ($d = 2$), on the other hand, forward scattering is relevant in this limit if $K_s < 2 + \sqrt{3}$. The generic case described by Eq. (18) is again very complicated to analyze. However, at least for simple microscopic models and in the limit of weak interactions where the rotation parameters can be calculated explicitly [see Eqs. (A7) and (A8) in the Appendix], we find that forward scattering is always relevant for $d = 2$.

The potential backscattering equations are, for the two spin channels,

$$\frac{dg_{b\sigma}}{dl} = g_{b\sigma}\Big[d - \underbrace{\tfrac{1}{2}\big[(\tilde{T}_1^{\phi} \pm T_1^{\phi})^2 + (\tilde{T}_2^{\phi} \pm T_2^{\phi})^2\big]}_{\equiv\gamma_{b\sigma}}\Big], \quad (19)$$

with the plus (minus) sign applying for $\sigma =\uparrow$ ($\sigma =\downarrow$). In the limit of $J \to 0$ we find $\gamma_{b\sigma} = [K_c + K_s]/2$. In the isotropic limit, $K_s \to 1$, this term is always relevant for repulsive interactions. In general, however, it can be either relevant or irrelevant. Indeed, it is also possible that potential backward scattering is relevant for one spin channel and irrelevant for the other.

The potential forward-scattering term has scaling dimension $x = 1$. It will therefore be relevant for an extended domain wall and marginal in the limit of a sharp wall.

As an example, we present in Fig. 3 the two scaling dimensions for forward and backward spin-flip scattering off an extended wall as a function of $\xi = J/2\varepsilon_F$ calculated for a U-V model with an on-site interaction $U/t = 1.10$ and nearest-neighbor interaction $V/t = 0.11$, where t is the hopping amplitude. Here the parameters of our low-energy effective model are determined in a lowest-order expansion in the interaction parameters. We want to remind the reader that by rotating back to the original physical model one finds that "spin-flip forward scattering" refers to an electron which passes through the wall *without* changing its spin.

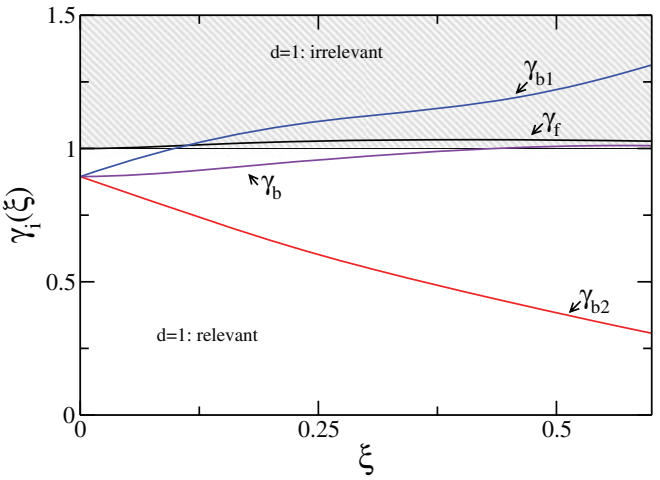

FIG. 3. (Color online) $\gamma_{f,b}$ and $\gamma_{b\sigma}$ for forward and backward, spin flip, and potential, scattering from an extended domain wall obtained for a specific U-V model (see text for details) as a function of $\xi = J/2\varepsilon_F$. The regions where the operators are relevant or irrelevant for $d = 1$ are marked. The condition $K_s = 1$ has been imposed by hand at the SU(2) symmetric point ($J = 0$) (see Appendix).

A. RG flow in the extended-domain-wall regime

At first we focus on the $d = 2$ case. For extended domain walls ($\lambda \gg \lambda_F$) the bare potential scattering terms $\sim(\lambda/\lambda_F)^2$ are much smaller than the spin-flip scattering terms $\sim(\lambda/\lambda_F)$. In the temperature range where it is appropriate to use the RG flow with $d = 2$ we can therefore neglect the potential scattering terms. They will, however, become important for the RG flow with $d = 1$ at even lower temperatures discussed in the next section.

Though with the physical parameters we consider in Sec. IV we find both $g_{f,b}$ to be relevant, by varying the $v_{c,s}$, $K_{c,s}$, and $v_{a,b}$ parameters we can find regimes where forward scattering remains relevant but backscattering becomes irrelevant.

We can now identify several regimes. We focus here first on the small magnetization limit close to half filling, where $\lambda_- \gg \lambda_+$. For the backward-scattering Hamiltonian, H^b_{Gsf} [Eq. (9)], this means that we take the limit where $k_{F\uparrow} \approx k_{F\downarrow} \to k_F \approx \pi/2$. We can then simplify (9) and find

$$H^b_{Gsf} = \frac{g_b}{2\pi m\alpha}\int dz\Theta'(z)\sin\big[\sqrt{2\pi}\theta_s(z)\big] \times \cos[2zk_F]\sin\big[\sqrt{2\pi}\phi_c(z)\big]. \quad (20)$$

We now consider the case that this term is relevant; i.e., g_b becomes large at low temperatures. First, for "narrow enough" walls, i.e., for domain walls of the order of the Fermi wavelength λ_F when the $2k_F$ oscillations do not cancel out the

contributions, then in order to minimize the energy the fields become locked over the length of the domain wall in the values $\{\phi_c = \sqrt{2\pi}(m+\frac{3}{4}), \theta_s = \sqrt{2\pi}(n+\frac{1}{4})\}$ or $\{\phi_c = \sqrt{2\pi}(m+\frac{1}{4}), \theta_s = \sqrt{2\pi}(n+\frac{3}{4})\}$ for integer m,n. Therefore, the domain wall becomes an impenetrable barrier for both charge and spin excitations and we find a spin-charge insulator.[18,37]

If we consider longer domain walls then, as already discussed previously, the effective bare coupling for backward scattering will be close to zero. Hence, for extended domain walls, $\lambda \gg \lambda_F$, forward scattering is always the more important because $\lambda_+ \ll \lambda_-$.

Therefore, there is also a regime in which only forward scattering is relevant: Either the long-domain-wall case or the case of irrelevant backward scattering ($\gamma_b > 2$). Considering again the limit of small magnetization and a system close to half filling, the forward-scattering term in Eq. (9) simplifies to

$$H^f_{Gsf} = \frac{g_f}{2\pi m\alpha}\int dz\Theta'(z)\sin[\sqrt{2\pi}\theta_s(z)] \times \cos[z(k_{F\uparrow}-k_{F\downarrow})]\sin[\sqrt{2\pi}\phi_s(z)]. \quad (21)$$

In order to minimize the energy in this case the fields become locked over the length of the domain wall in the values $\{\phi_s = \sqrt{2\pi}(m+\frac{3}{4}), \theta_s = \sqrt{2\pi}(n+\frac{1}{4})\}$ or $\{\phi_s = \sqrt{2\pi}(m+\frac{1}{4}), \theta_s = \sqrt{2\pi}(n+\frac{3}{4})\}$ for integer m,n. In this scenario only the spin sector is frozen out and we find a C1S0 phase where the spin mode is gapped but charge excitations remain gapless.[39] In the physical reference frame this is a state in which the incoming spin current does not scatter from the domain wall and, after traversing the domain wall, ends in the antiparallel spin configuration with respect to the bulk. This means that the domain-wall profile can no longer be taken as adiabatic.

From the above considerations we have several possibilities. First, we can have backward scattering as either relevant or irrelevant. Second, we must consider the relative length scales. If $\lambda_+ < \lambda$ then the backward-scattering terms are small due to averaging over their oscillations. A similar case holds for the forward scattering with $\lambda_+ \to \lambda_-$ in the preceding. For the case in which both the forward- and the backward-scattering length scales are shorter than the domain-wall length we end up in the completely adiabatic limit, as one would expect, and the system shows LL properties ("adiabatic LL"). Again we note that at extremely low temperatures we have to switch to a $d = 1$ RG flow and backward-scattering processes will begin to dominate and can lead to insulating regimes. In principle, we can also be in the opposite regime when both forward- and backward-scattering length scales are longer than the domain-wall length, in which case the scaling dimensions of the forward- and backward-scattering terms alone determine what the low-energy fixed point is. Note that this is possible without requiring a very sharp δ-function-like domain-wall profile. In general, however, the low-temperature phase the system ends up in in the extended regime depends not only on the relevance of the operators, but also on the hierarchy of length scales.

The different behaviors in the extended regime which could be identified from the first-order RG equations are summarized in Table I. Finally, let us also comment on the case of a generic magnetization and arbitrary filling. In this case the analysis above stays valid, the spin and charge modes, however, get locked into more complicated spin- and charge-density wave states over the length of the domain wall.

TABLE I. The different phases of the ferromagnetic LL with an extended domain wall ($d = 2$, relevant spin-flip forward scattering) depending on the scaling dimensions of the spin-flip backward scattering operator *and* the hierarchy of the three length scales present in the problem.

	$\lambda \lesssim \lambda_\pm$	$\lambda_+ < \lambda < \lambda_-$	$\lambda_\pm < \lambda$
$2-\gamma_b > 0$	Spin and charge insulator	C1S0	Adiabatic LL
$2-\gamma_b < 0$	C1S0	C1S0	Adiabatic LL

B. Fixed points of the $d = 1$ sharp-domain-wall regime

For the case of a very sharp domain wall ($d = 1$) we have shown that forward spin-flip scattering is always irrelevant. The forward potential scattering term is marginal and we ignore it as well. In this case the possible phases are therefore determined by the scaling dimensions of the two backward-scattering terms alone. (Naturally, for a sharp wall the length scales can play no further role.) Formally, one can find the sharp domain-wall limit from Eq. (2) by taking the limit $\lambda \to 0$, which requires $\Theta'(z) \to \pi\delta(z)$. This leads to an effective model where all the boundary scattering terms allowed by symmetry are present. A full description of the phase space for this model with different relevant perturbations present requires the solution to the second-order RG equations to find the separatrix between the different low-temperature fixed points. The second-order equation for our model is more complicated than for the standard sine-Gordon model. A diagonal equation in the ϕ_i's is not recovered and to perform any further analysis we would have to rediagonalize the problem and then renormalize the model once again, repeating these steps until we reached the fixed point.[38] This is perhaps not totally unexpected as the scattering terms we are dealing with explicitly couple the normal modes. We leave the more involved second-order RG analysis to a future work and focus here on what the first-order equations can tell us. The flow of a similar model has already been analyzed by Araújo *et al.*[16,17] using poor man's scaling. In that work they consider both spin-flip and pure potential backscattering from a sharp domain wall, treating the interaction only perturbatively. They find phases dominated by the spin-flip and pure potential backscattering processes. In contrast Pereira and Miranda[18] consider only the spin-flip backscattering term and hence cannot recover all possible low-energy phases.

There are three possible fixed points of the RG flow depending on the relative relevance of the three backscattering channels, g_b, $g_{b\uparrow}$, and $g_{b\downarrow}$. The system can flow to a spin and charge insulator, an effectively spinless LL, or a spin-full LL. Furthermore, the spin and charge insulator itself can show different physical behavior in the region of the domain wall depending on the relative relevance of the backscattering operators. This behavior will be confined to some region around the boundary. First, let us discuss the spin- and charge-insulating phase. If the pure potential backscattering for both

TABLE II. The different phases of the ferromagnetic LL with an effectively sharp domain wall ($d = 1$, irrelevant forward scattering) depending on the relevance or irrelevance of the backward-scattering operators. The physics of the system surrounding the domain wall for the spin- and charge-insulating phase depends upon the relative relevance of the backward-scattering operators and is discussed fully in the text.

$\gamma_b < 1$ and/or $\gamma_{b\uparrow},\gamma_{b\downarrow} < 1$	$\gamma_{b\sigma} < 1$ $\gamma_b,\gamma_{b\bar{\sigma}} > 1$	$\gamma_b > 1$ $\gamma_{b\uparrow},\gamma_{b\downarrow} > 1$
Spin and charge insulator	Effective spinless LL	LL

spin channels is relevant and dominates, $\gamma_{b\sigma} < \gamma_b$, then the system will flow to the spin- and charge-insulating fixed point already studied by Kane and Fisher[5] with the spin part of the system remaining completely unaffected. If the spin-flip backscattering term is relevant and dominates, $\gamma_b < \gamma_{b\sigma}$, then we have the fixed point analyzed by Pereira and Miranda.[18] The spin-flip back scattering will tend to equilibriate the number of up and down spins. This fixed point must therefore correspond physically to a spin and charge insulator with a region of reduced spin polarization around the boundary. It is also possible to have the situation where $\gamma_{b\sigma} < \gamma_b < \gamma_{b\bar{\sigma}}$ with $\gamma_{b\sigma},\gamma_b < 1$. In this case as the system approaches the fixed point first one spin channel will become insulating; however, before the second spin channel also becomes insulating the spin-flip backscattering term will tend to align the spins into the first channel. Once the spins are scattered into the first channel they are more likely to be scattered without a spin flip than back into the other spin channel. Therefore, the final fixed point will likely be an insulator with a region of increased spin polarization around the domain wall. Second, if potential back scattering is relevant for one channel but irrelevant for the other and spin-flip scattering is irrelevant as well, then we are left with an effective spinless LL; i.e., we have one insulating and one conducting channel. Finally, if all back-scattering operators are irrelevant, then the system remains a LL.

These results are summarized in Table II.

IV. SPIN AND CHARGE DENSITY IN THE PERTURBATIVE REGIME

We now return to the case of an extended domain wall, $\lambda \gg \lambda_F$, where the potential scattering terms can be ignored and consider a perturbative temperature regime where the spin-flip scattering terms can be treated perturbatively. This allows us to calculate the spin and charge densities around the domain wall. Spin- and charge-density oscillations around impurities are not only experimentally relevant, but also provide a useful theoretical tool to analyze the dominant physical scattering processes in general low-dimensional strongly correlated systems.[40–43] As we are interested in the case where both forward and backward scattering are relevant perturbations, a perturbative treatment of the scattering terms will break down at low-enough temperatures. We indeed find that the perturbative corrections increase as a power law in inverse temperature. In order for perturbation theory to be valid, we find that the following conditions, for forward- and backward-scattering terms respectively, have to be held:

$$\left(\frac{T}{T_1^*}\right)^{\alpha_1}\left(\frac{T}{T_2^*}\right)^{\alpha_2} \ll \frac{4\pi\lambda m T}{g_f\left[T_1^\phi T_1^\theta + T_2^\phi T_2^\theta\right]} \tag{22}$$

and

$$\left(\frac{T}{T_1^*}\right)^{\beta_1}\left(\frac{T}{T_2^*}\right)^{\beta_2} \ll \frac{4\pi\lambda m T}{g_b\left[T_1^\phi T_1^\theta + T_2^\phi T_2^\theta\right]}. \tag{23}$$

Here $T_i^* \sim u_i/(2\pi\alpha)$ is a cutoff scale and the exponents are given by $\alpha_i = [(T_i^\phi)^2 + (T_i^\theta)^2]/4$ and $\beta_i = [(\tilde{T}_2^\phi)^2 + (T_2^\theta)^2]/4$. Note that $\alpha_1 + \alpha_2 = \gamma_f/2$ and $\beta_1 + \beta_2 = \gamma_b/2$ so that the scaling dimensions show up in Eqs. (22) and (23) in the expected way.

We want to present our results in the physical unrotated frame. The perturbative results are, however, obtained in the rotated frame so that we have to use the gauge transformation $\mathbf{U}(z)$ once more. The spin density, in the physical frame, is

$$\vec{S}(z) = \tfrac{1}{2}\tilde{\boldsymbol{\psi}}^\dagger(z)\vec{\boldsymbol{\sigma}}\tilde{\boldsymbol{\psi}}(z) = \tfrac{1}{2}\boldsymbol{\psi}^\dagger(z)\underbrace{\boldsymbol{U}^\dagger\vec{\boldsymbol{\sigma}}\boldsymbol{U}}_{\vec{\boldsymbol{\sigma}}'}\boldsymbol{\psi}(z), \tag{24}$$

where the gauge rotated Pauli matrices are given explicitly by

$$\begin{aligned}\boldsymbol{\sigma}'_x &= \boldsymbol{\sigma}^x,\\ \boldsymbol{\sigma}'_y &= \cos[\Theta(z)]\boldsymbol{\sigma}^y - \sin[\Theta(z)]\boldsymbol{\sigma}^z,\\ \boldsymbol{\sigma}'_z &= \sin[\Theta(z)]\boldsymbol{\sigma}^y + \cos[\Theta(z)]\boldsymbol{\sigma}^z.\end{aligned} \tag{25}$$

Using these relations, the spin densities in the physical frame $\vec{S}(z)$ can now be constructed from the spin densities $\vec{S}_0(z) = \frac{1}{2}\boldsymbol{\psi}^\dagger(z)\vec{\boldsymbol{\sigma}}\boldsymbol{\psi}(z)$ in the rotated frame. The corrections to the bulk in first order in forward and backward scattering off the domain wall are given by

$$\begin{aligned}\left\langle \Delta S_0^x(z)\right\rangle = \frac{1}{\alpha\pi}\langle &\cos[\sqrt{2\pi}\theta_s(z)]\\ &\times[\cos[(k_{F\uparrow}-k_{F\downarrow})z + \sqrt{2\pi}\phi_s(z)]\\ &+\cos[(k_{F\uparrow}+k_{F\downarrow})z + \sqrt{2\pi}\phi_c(z)]]\rangle,\end{aligned} \tag{26}$$

$$\begin{aligned}\left\langle \Delta S_0^y(z)\right\rangle = \frac{1}{\alpha\pi}\langle &\sin[\sqrt{2\pi}\theta_s(z)]\\ &\times[\cos[(k_{F\uparrow}-k_{F\downarrow})z + \sqrt{2\pi}\phi_s(z)]\\ &+\cos[(k_{F\uparrow}+k_{F\downarrow})z + \sqrt{2\pi}\phi_c(z)]]\rangle, \quad \text{and}\end{aligned} \tag{27}$$

$$\begin{aligned}\left\langle \Delta S_0^z(z)\right\rangle = \Bigg\langle &-\frac{1}{\sqrt{2\pi}}\partial_z\phi_s(z)\\ &+\frac{1}{2\alpha\pi}\sum_\sigma \sigma^z_{\sigma\sigma}\cos[2xk_{F\sigma} - 2\sqrt{\pi}\phi_\sigma(z)]\Bigg\rangle.\end{aligned} \tag{28}$$

Note that in the linearization procedure, strictly speaking, we should write $\psi_\sigma(z) = \psi_{0\sigma}(z) + e^{ik_{F\sigma}z}\psi_{\sigma+}(z) + e^{-ik_{F\sigma}z}\psi_{-\sigma}(z)$. These $\boldsymbol{\psi}_0^\dagger(z)\vec{\boldsymbol{\sigma}}\boldsymbol{\psi}_0(z)$ terms missing from the above spin densities give the bulk values. We can also use a description where we absorb the effective magnetic field by a shift in the bosonic fields instead of linearizing around the spin-split Fermi points. In this case, however, we must take

into account curvature terms.[44] This would reintroduce the bulk spin-density terms explicitly in Eqs. (26) to (28).

In the following, we want to consider two examples. Example (a) corresponds to a case where $\lambda_+ \ll \lambda < \lambda_-$ so that only forward scattering contributes. In example (b), on the other hand, we consider the case $\lambda_+ \ll \lambda_- \lesssim \lambda$ so that forward scattering is again dominant but is oscillating over the length of the domain wall. More specifically, we consider values which are appropriate for Fe, $\lambda_F = 0.367$ nm, and a lattice cutoff $\alpha = \lambda_F$. We plot results for two sets of parameters: (a) $\frac{J}{2} = 0.112$ eV, $\lambda = 10\lambda_F$, and $T = 25$ K; and (b) $\frac{J}{2} = 2.23$ eV, $\lambda = 10\lambda_F$, and $T = 50$ K. These parameters give us the following scaling terms: (a) $\gamma_f = 1.12$ and $\gamma_b = 0.923$; and (b) $\gamma_f = 1.09$ and $\gamma_b = 0.937$. In both cases the conditions (22) and (23) are fulfilled with the ratio of the right-hand side divided by the left-hand side being of the order 10^{-3} for the condition on backward scattering [Eq. (23)] and of the order 10^{-1} for forward scattering [Eq. (22)].

Figures 4 and and 5 show the spin density around the domain wall, normalized to the average value per conduction electron, $S = \frac{1}{2}$. For the situation where the length scale of the forward-scattering oscillations is larger than the domain-wall length, case (a), the spin-density profile is significantly altered [see Figs. 4(a) and 5(a)]. Such a shift will affect how the domain wall itself behaves in the effective magnetic field applied by

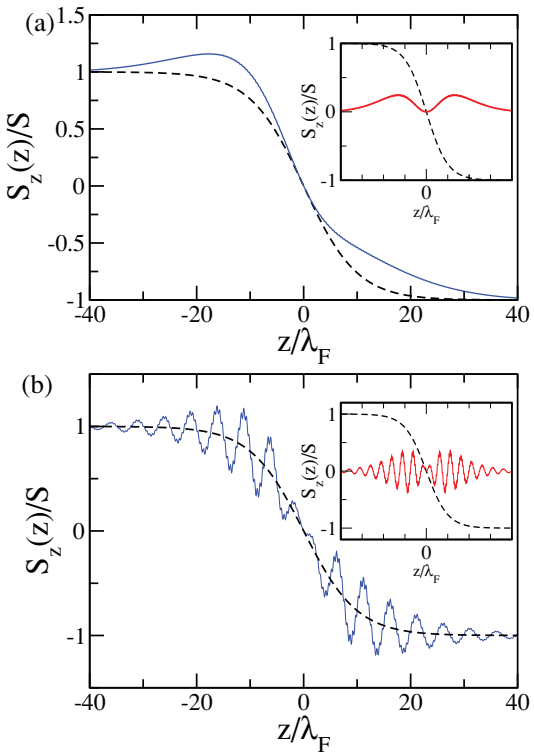

FIG. 4. (Color online) The spin density $S_z(z)/S$, showing the zeroth-order (dashed line) term and the total value (blue solid line). The inset shows a comparison of the the zeroth-order (dashed line) and first-order (red solid line) terms. Zeroth and first order refer to an expansion in the scattering potential. All the spin figures are normalized to the average value per conduction electron, $S = \frac{1}{2}$. The domain-wall length is $\lambda = 10\lambda_F$ with (a) $\frac{J}{2} = 0.112$ eV and $T = 25$ K and (b) $\frac{J}{2} = 2.23$ eV and $T = 50$ K.

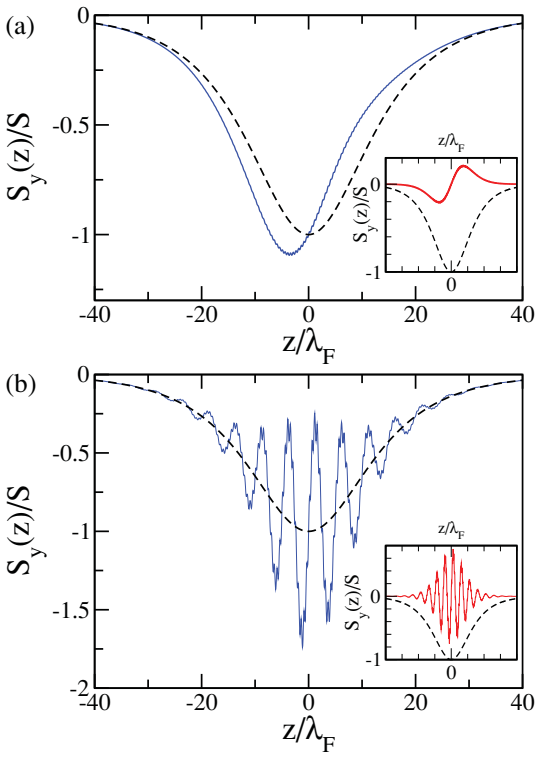

FIG. 5. (Color online) Same as Fig. 4 but for the spin density $S_y(z)/S$.

the conduction electrons and therefore will strongly affect the domain-wall dynamics. As expected, the backward scattering plays no role in the considered temperature range.

The asymmetric distortion of the spin density clearly visible in Figs. 4(a) and 5(a) is due to the addition of antisymmetric and symmetric combinations of the spin densities. In contrast to Figs. 4(b) and 5(b), where the Friedel oscillations are rapid when compared to the domain-wall length, here the Friedel oscillations from forward scattering are on a longer length scale than λ. Hence, the changes in the spin density they cause can be seen as an overall distortion in its profile.

When both λ_+ and λ_- are smaller than the domain-wall length [see Figs. 4(b) and 5(b)], oscillations within the overall domain-wall profile are clearly visible. Here the long wavelength oscillations are caused by forward scattering while the much faster oscillating backward-scattering term causes the small "wiggles" on top of the oscillations. In this case the overall spin-density profile is not shifted.

The first-order charge-density correction, derived similarly, is given by

$$\langle \Delta\rho(z)\rangle = e\Big\langle -\sqrt{\frac{2}{\pi}}\partial_z\phi_c(z) + \frac{1}{\alpha\pi}\sum_\sigma \cos[2zk_{F\sigma} - 2\sqrt{\pi}\phi_\sigma(z)]\Big\rangle. \quad (29)$$

The main contribution to the charge density can be calculated analytically and can be found in the Appendix [Eq. (A11)]. Results for cases (a) and (b) are shown in Fig. 6. In case (a) we do see a charge buildup, and respectively depletion,

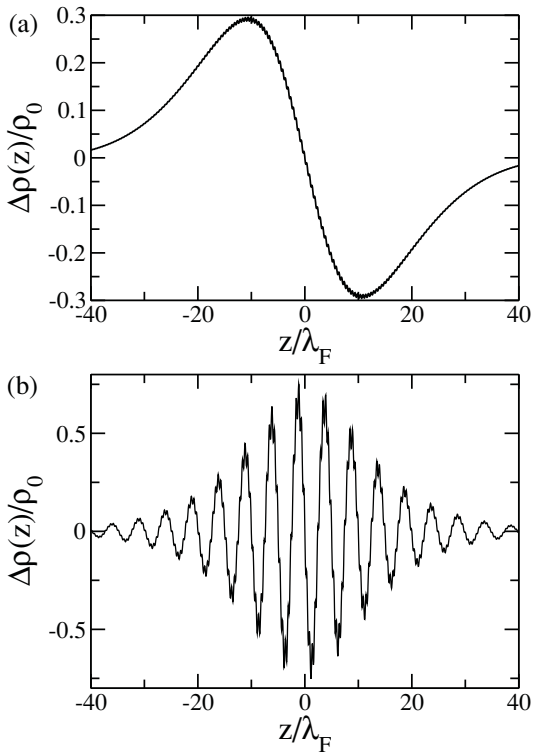

FIG. 6. The charge-density correction, $\Delta\rho(z)$, per electron per unit cell: $\rho_0 = 2e/\alpha \mathrm{Cm}^{-1}$. The domain-wall length is $\lambda = 10\lambda_F$ with parameters for panels (a) and (b) as given in Fig. 4.

antisymmetric with respect to the center of the domain wall. The small "wiggles" on top of the overall charge rearrangement are caused by backward scattering. In case (b) we see strong oscillations of the charge density caused by forward scattering which are largest at the center of the domain wall. The very fast oscillations, which can be seen in more detail in Fig. 7, originate from backscattering. Finally, we note that the overall charge in the model is conserved; i.e., $\int dz \Delta\rho(z) = 0$. The total spin $\langle S^2 \rangle$ in the system is also conserved and is related to the charge density: $\langle S^2(z) \rangle = \frac{3}{4e} \langle \rho(z) \rangle$. Therefore, the total spin is redistributed throughout the wire in precisely the same way as the charge. However, none of S^x, S^y, or S^z are themselves conserved.

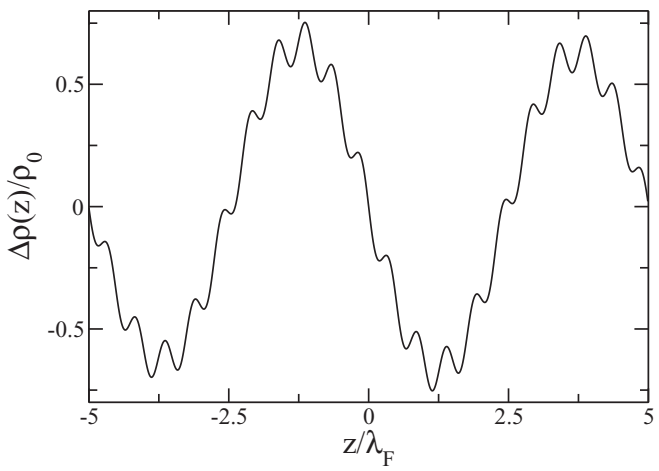

FIG. 7. Same as Fig. 6(b) where we have zoomed in on a shorter length making the oscillations due to backscattering clearly visible.

If we compare Fig. 6 to the results found by Dugaev *et al.*,[15] the most striking difference is the presence of strong Friedel oscillations. Such oscillations are well known and are already present in the noninteracting case. However, we also see that depending on parameters the amplitude of the Friedel oscillations can be quite small [see, e.g., Fig. 6(a)] and might be easily overlooked if one mainly concentrates on the overall shape. Compared to the noninteracting case[45] the spin-density corrections have a different profile around the domain wall in the transverse direction. We want to stress that our model offers a method of calculating *nonperturbatively* the full effect of short-range electron-electron interactions on any physical property we are interested in. Provided, of course, that one is in the regime of sufficiently high temperatures such that the perturbative analysis of the gauge potential remains valid. This includes, in particular, the physically important regime for quantum wires in ferromagnetic materials discussed above. In such systems, however, the phases of the extended domain-wall regime (see Table I) should also be accessible.

We now want to briefly discuss consequences of the strong correlations in the electronic systems for the dynamics of the domain wall. The magnetization dynamics are described by the Landau-Lifschitz-Gilbert (LLG) equation, or some suitable generalization thereof.[46–48] There are two different aspects to this we must consider. One is the straightforward point that the dynamics, *over the length of the wall*, will be affected by the different spin density of the LL compared to the Fermi liquid or noninteracting case. The second, more interesting, point is whether the derivation of the nonadiabatic terms in the LLG equation are valid for a LL.

Following Zhang and Li[48] one can derive contributions to the magnetization dynamics which allow for the fact that the electrons do not instantaneously follow the magnetization profile. One first writes a continuity equation for the spins, assuming part of it to be always parallel to the bulk magnetization and allowing a small deviation from this. In order to derive the current-dependent (so-called β-) terms, those which drive the domain wall along the wire, one assumes that $j_s^{x,y,z}(z,t) = -\mu_B P j_e^{x,y,z}(z,t) n^{x,y,z}(z,t)/e$. $\vec{j}_e(z,t)$ is the charge current and P is the magnitude of the polarization, while $\vec{j}_s(z,t)$ is the spin current. A quite reasonable assumption in a Fermi liquid, this of course starts to look more dubious in the case of a LL. In the standard LL model spin and charge are, of course, uncorrelated and possess different velocities. Thus, this assumption would completely fail. For us the situation is not so simple as we do not have spin-charge separation, nonetheless what is obvious from our model is that spin and charge are not fully correlated. One is forced to work with the spin current and not the electric current and, as we have already seen, the spin degrees of freedom can behave rather differently for this model.

V. CONCLUSION

We have investigated a LL coupled to a noncollinear ferromagnetic magnetization profile in the shape of a domain wall. The domain wall acts as a spatially extended magnetic

impurity for the electrons and introduces both forward- and backward-scattering terms, active over the length of the domain wall. In contrast to the well-studied case of pointlike impurities in LLs the finite extent of the domain wall introduces a whole new layer of complexity to the problem. In a RG treatment of the scattering terms, one has to distinguish between an extended regime and a sharp regime at low temperatures where the domain wall effectively becomes a δ function. In the extended regime the scattering terms are bulk operators while they become boundary operators in the sharp regime. An operator relevant in the extended regime can therefore become irrelevant in the sharp regime.

Simplest to understand is the sharp regime. Here the spin-flip and potential forward-scattering terms are irrelevant or marginal, respectively. The low-temperature fixed points are then determined by the spin-flip and potential backscattering terms both of which can be either relevant or irrelevant. If both are irrelevant, then the fixed point is the LL; if potential back scattering is only relevant for one spin channel with the other terms being irrelevant, then the fixed point is an effective spinless LL. In all other cases the fixed-point will be a spin and charge insulator. Depending on the relative relevance of the backscattering operators, the region of the insulator in the vicinity of the domain wall can show a reduced, increased or unaffected polarization in comparison to the bulk.

If we start with an extended domain wall, however, then the domain-wall length λ will usually be large compared to the backward-scattering length λ_+; i.e., the backward-scattering terms will strongly oscillate over the length of the domain wall. This means that the effective bare coupling—roughly proportional to the Fourier mode of the domain-wall potential commensurate with the backward-scattering oscillations—will be exponentially small $\sim \exp(-\lambda/\lambda_+)$. So even if backward scattering is relevant, temperatures $T/J < \exp(-\lambda/\lambda_+)$ are required in order to make this scattering process important. The sharp regime is therefore only physically relevant if we already start with a very sharp domain wall (of the order of a few lattice sites) which could possibly be realized by a nanoconstriction.

In the extended regime, the low-temperature physics of the model is not only determined by the relevance or irrelevance of the various scattering terms but also by the hierarchy of the three different length scales present in the problem. Analyzing the first-order RG equations for backward and forward scattering and taking the hierarchy of the three length scales into account we could identify three phases. If both the scattering terms are irrelevant or they are relevant but the associated length scales are much smaller than the domain-wall length λ, we find an adiabatic Luttinger liquid. In this case the spins of the electrons follow the magnetization profile and both charge and spin excitations are gapless. If both scattering terms are relevant and their respective length scales larger than λ then the first-order RG equations suggest that the system will become a spin-charge insulator; i.e., the domain wall will act as a perfectly reflecting barrier. This case corresponds to the normal Kane-Fisher fixed point. Finally, there is the case of forward scattering being relevant and the associated length scale being larger than λ, with backward scattering being either irrelevant or having an associated length scale which is smaller than λ. In this case the charge modes are gapless and charge is allowed to pass through the domain-wall barrier. The spin modes, on the other hand, are locked to a specific value over the length of the domain wall and the system becomes insulating with respect to spin transport (C1S0 phase). Physically, this means that electrons no longer undergo a change of spin on passing through the domain wall. The latter phase has not been discussed so far in this context and it is this phase which we believe is most important in possible experimental realizations.

We also calculated the spin and charge densities around the domain wall for physically reasonable parameters in a regime at high-enough temperatures so that even relevant scattering terms can be treated perturbatively. Here one finds spin and charge distributions markedly different from the previously reported mean-field interaction case. Both the overall profile and the local distribution of spin and charge show different behavior, including Friedel oscillations. A similar result to ours for the lateral component of spin is found in the noninteracting case,[45] though the transverse components look qualitatively different. As an outlook, we believe that it will be interesting to study how the dynamics of the domain wall is changed in this temperature range where correlation effects dramatically alter the spin and charge densities compared to the noninteracting case but where we are still far above the phase transition temperatures to the low-temperature phases discussed above.

ACKNOWLEDGMENTS

The authors wish to thank both J. Berakdar and R. G. Pereira for useful and stimulating discussions. This work was supported by the DFG via the SFB/Transregio 49 and the MAINZ (MATCOR) graduate school of excellence.

APPENDIX: DETAILS OF THE ROATATIONS

The spin and charge Luttinger parameters are, to lowest orders,

$$\begin{aligned}
v_c &= \frac{v_{F\uparrow}+v_{F\downarrow}}{2}+\frac{g_{4\parallel\uparrow}+g_{4\parallel\downarrow}+2g_{4\perp}}{4\pi},\\
v_s &= \frac{v_{F\uparrow}+v_{F\downarrow}}{2}+\frac{g_{4\parallel\uparrow}+g_{4\parallel\downarrow}-2g_{4\perp}}{4\pi},\\
K_c &= 1-\frac{1}{2\pi}\frac{g_{2\parallel\uparrow}+g_{2\parallel\downarrow}+2g_{2\perp}}{v_{F\uparrow}+v_{F\downarrow}},\\
K_s &= 1-\frac{1}{2\pi}\frac{g_{2\parallel\uparrow}+g_{2\parallel\downarrow}-2g_{2\perp}}{v_{F\uparrow}+v_{F\downarrow}},\\
v_a &= \frac{v_{F\uparrow}-v_{F\downarrow}}{2}-\frac{g_{2\parallel\uparrow}-g_{2\parallel\downarrow}}{4\pi}+\frac{g_{4\parallel\uparrow}-g_{4\parallel\downarrow}}{4\pi}, \quad \text{and}\\
v_b &= \frac{v_{F\uparrow}-v_{F\downarrow}}{2}+\frac{g_{2\parallel\uparrow}-g_{2\parallel\downarrow}}{4\pi}+\frac{g_{4\parallel\uparrow}-g_{4\parallel\downarrow}}{4\pi}.
\end{aligned} \tag{A1}$$

In order to enforce the condition $K_s = 1$ at the SU(2) symmetric point ($J = 0$) we set

$$K_s = 1-\frac{1}{2\pi}\frac{g_{2\parallel\uparrow}+g_{2\parallel\downarrow}}{v_{F\uparrow}+v_{F\downarrow}}, \tag{A2}$$

canceling the $g_{2\perp}$ term by hand. It is clear that this J independent term must cancel when higher-order corrections

are included. What we do not know in this low-order analysis is how the J dependence of the Luttinger parameters will be modified by higher-order terms.

The two rotations we use on the bosonic fields are

$$\begin{pmatrix}\phi_\uparrow\\ \phi_\downarrow\\ \theta_\uparrow\\ \theta_\downarrow\end{pmatrix} = \underbrace{\frac{1}{\sqrt{2}}\begin{pmatrix}-1&0&-1&0\\0&-1&0&-1\\1&0&-1&0\\0&1&0&-1\end{pmatrix}}_{=\mathcal{U}^{-1}}\begin{pmatrix}\phi_{\uparrow+}\\ \phi_{\downarrow+}\\ \phi_{\uparrow-}\\ \phi_{\downarrow-}\end{pmatrix} \tag{A3}$$

and

$$\begin{pmatrix}\phi_s\\ \phi_c\\ \theta_s\\ \theta_c\end{pmatrix} = \underbrace{\frac{1}{\sqrt{2}}\begin{pmatrix}1&-1&0&0\\1&1&0&0\\0&0&1&-1\\0&0&1&1\end{pmatrix}}_{=\tilde{\mathcal{U}}^{-1}}\begin{pmatrix}\phi_\uparrow\\ \phi_\downarrow\\ \theta_\uparrow\\ \theta_\downarrow\end{pmatrix}. \tag{A4}$$

To diagonalize the matrix $\tilde{M}$ [Eq. (8)], we perform two steps. The first is a rotation to make the Hamiltonian diagonal, characterized by the $R^{\theta,\phi}_{1,2}$ terms. The second is a rescaling to leave us with two distinct eigenvalues rather than four; this introduces the Γ's. Together this gives us

$$\begin{pmatrix}\theta_1(z)\\ \theta_2(z)\end{pmatrix} = \begin{pmatrix}R^\theta_1\sqrt{\Gamma^\theta_1} & R^\theta_2\sqrt{\Gamma^\theta_1}\\ -R^\theta_2\sqrt{\Gamma^\theta_2} & R^\theta_1\sqrt{\Gamma^\theta_2}\end{pmatrix}\begin{pmatrix}\theta_c(z)\\ \theta_s(z)\end{pmatrix} \quad \text{and}$$
$$\begin{pmatrix}\phi_1(z)\\ \phi_2(z)\end{pmatrix} = \begin{pmatrix}R^\phi_1\sqrt{\Gamma^\phi_1} & R^\phi_2\sqrt{\Gamma^\phi_1}\\ -R^\phi_2\sqrt{\Gamma^\phi_2} & R^\phi_1\sqrt{\Gamma^\phi_2}\end{pmatrix}\begin{pmatrix}\phi_c(z)\\ \phi_s(z)\end{pmatrix}. \tag{A5}$$

Here the rotation components are

$$2\left(R^\theta_{1,2}\right)^2 = 1 \pm \left[1 + \frac{v_a^2}{\left(\frac{v_cK_c}{2} - \frac{v_sK_s}{2}\right)^2}\right]^{-\frac{1}{2}} \quad \text{and}$$
$$2\left(R^\phi_{1,2}\right)^2 = 1 \pm \left[1 + \frac{v_b^2}{\left(\frac{v_c}{2K_c} - \frac{v_s}{2K_s}\right)^2}\right]^{-\frac{1}{2}}. \tag{A6}$$

In order for the rotated Hamiltonian to have positive eigenvalues the condition $v_cv_s/v_b^2 > K_cK_s > v_a^2/v_cv_s$ must also be satisfied. This condition seems to be always fulfilled, at least if one uses the integrable Hubbard model as the underlying microscopic lattice model.[11]

The rescaling of the fields requires

$$\left(\Gamma^\phi_{1,2}\right)^2 = \left(\Gamma^\theta_{1,2}\right)^{-2} \quad \text{and}$$
$$\left(\Gamma^\phi_{1,2}\right)^2 = \frac{\frac{v_c}{2K_c} + \frac{v_s}{2K_s} \pm \sqrt{v_b^2 + \left(\frac{v_c}{2K_c} - \frac{v_s}{2K_s}\right)^2}}{\frac{v_cK_c}{2} + \frac{v_sK_s}{2} \pm \sqrt{v_a^2 + \left(\frac{v_cK_c}{2} - \frac{v_sK_s}{2}\right)^2}}. \tag{A7}$$

Note that as the rotation is a unitary transformation we have the condition $[R^{\theta,\phi}_1]^2 + [R^{\theta,\phi}_2]^2 = 1$. For our convenience we finally define

$$T^{\theta,\phi}_1 = R^{\theta,\phi}_2/\sqrt{\Gamma^{\theta,\phi}_1}, \quad T^{\theta,\phi}_2 = R^{\theta,\phi}_1/\sqrt{\Gamma^{\theta,\phi}_2},$$
$$\tilde{T}^{\theta,\phi}_1 = R^{\theta,\phi}_1/\sqrt{\Gamma^{\theta,\phi}_1}, \quad \text{and} \quad \tilde{T}^{\theta,\phi}_2 = -R^{\theta,\phi}_2/\sqrt{\Gamma^{\theta,\phi}_2}. \tag{A8}$$

Therefore, the inverse of Eq. (A5) is

$$\begin{pmatrix}\phi_c(z)\\ \phi_s(z)\end{pmatrix} = \begin{pmatrix}\tilde{T}^\phi_1 & \tilde{T}^\phi_2\\ T^\phi_1 & T^\phi_2\end{pmatrix}\begin{pmatrix}\phi_1(z)\\ \phi_2(z)\end{pmatrix} \quad \text{and}$$
$$\begin{pmatrix}\theta_c(z)\\ \theta_s(z)\end{pmatrix} = \begin{pmatrix}\tilde{T}^\theta_1 & \tilde{T}^\theta_2\\ T^\theta_1 & T^\theta_2\end{pmatrix}\begin{pmatrix}\theta_1(z)\\ \theta_2(z)\end{pmatrix}. \tag{A9}$$

Finally, the values of the new eigenvalues are

$$u^2_{1,2} = \left(\frac{v_c}{2K_c} + \frac{v_s}{2K_s} \pm \sqrt{v_b^2 + \left(\frac{v_c}{2K_c} - \frac{v_s}{2K_s}\right)^2}\right) \times \left(\frac{v_cK_c}{2} + \frac{v_sK_s}{2} \pm \sqrt{v_a^2 + \left(\frac{v_cK_c}{2} - \frac{v_sK_s}{2}\right)^2}\right). \tag{A10}$$

As expected this reduces directly to the spin and charge excitation velocities in the absence of spin asymmetry. In such a case the Hamiltonian is already diagonal and the above rotation is no longer necessary.

The analytical result for the charge-density correction is

$$\langle\Delta\rho(z)\rangle = \frac{e\,\mathrm{sech}[z/\lambda]}{2\pi mT\alpha\lambda}\left[T^\phi_1T^\theta_1 + T^\phi_2T^\theta_2\right] \times \left[g_f\sin[z/\lambda_-]\left(\frac{T}{T^*_1}\right)^{\alpha_1}\left(\frac{T}{T^*_2}\right)^{\alpha_2} + g_b\sin[z/\lambda_+]\left(\frac{T}{T^*_1}\right)^{\beta_1}\left(\frac{T}{T^*_2}\right)^{\beta_2}\right]. \tag{A11}$$

*sedlmayr@physik.uni-kl.de

[1] S. Tomonaga, Prog. Theor. Phys. **5**, 544 (1950).
[2] J. M. Luttinger, J. Math. Phys. **4**, 1154 (1963).
[3] T. Giamarchi, *Quantum Physics in One-Dimension* (Oxford University Press, Oxford, 2003).
[4] C. L. Kane and M. P. A. Fisher, Phys. Rev. Lett. **68**, 1220 (1992).
[5] C. L. Kane and M. P. A. Fisher, Phys. Rev. B **46**, 15233 (1992).
[6] S. Eggert and I. Affleck, Phys. Rev. B **46**, 10866 (1992).
[7] S. Eggert and I. Affleck, Phys. Rev. Lett. **75**, 934 (1995).
[8] S. Rommer and S. Eggert, Phys. Rev. B **62**, 4370 (2000).
[9] J. Sirker, N. Laflorencie, S. Fujimoto, S. Eggert, and I. Affleck, Phys. Rev. Lett. **98**, 137205 (2007).
[10] J. Sirker, S. Fujimoto, N. Laflorencie, S. Eggert, and I. Affleck, J. Stat. Mech.: Theory Exp. (2008) P02015.
[11] K. Penc and J. Sólyom, Phys. Rev. B **47**, 6273 (1993).
[12] H. Frahm and V. E. Korepin, Phys. Rev. B **43**, 5653 (1991).
[13] C. H. Marrows, Adv. Phys. **54**, 585 (2005).
[14] S. S. P. Parkin, M. Hayashi, and L. Thomas, Science **320**, 190 (2008).
[15] V. K. Dugaev, J. Barnaś, A. Łusakowski, and L. A. Turski, Phys. Rev. B **65**, 224419 (2002).
[16] M. A. N. Araújo, V. K. Dugaev, V. R. Vieira, J. Berakdar, and J. Barnaś, Phys. Rev. B **74**, 224429 (2006).

[17]M. A. N. Araújo, J. Berakdar, V. K. Dugaev, and V. R. Vieira, Phys. Rev. B **76**, 205107 (2007).
[18]R. G. Pereira and E. Miranda, Phys. Rev. B **69**, 140402 (2004).
[19]P. Bruno, Phys. Rev. Lett. **83**, 2425 (1999).
[20]P. Gambardella, A. Dallmeyer, K. Maiti, M. C. Malagoli, W. Eberhardt, K. Kern, and C. Carbone, Nature (London) **416**, 301 (2002).
[21]J. Shen, R. Skomski, M. Klaua, H. Jenniches, S. S. Manoharan, and J. Kirschner, Phys. Rev. B **56**, 2340 (1997).
[22]H. J. Elmers, J. Hauschild, H. Höche, U. Gradmann, H. Bethge, D. Heuer, and U. Köhler, Phys. Rev. Lett. **73**, 898 (1994).
[23]J. Hauschild, H. J. Elmers, and U. Gradmann, Phys. Rev. B **57**, R677 (1998).
[24]R. Wiesendanger, Rev. Mod. Phys. **81**, 1495 (2009).
[25]N. D. Mermin and H. Wagner, Phys. Rev. Lett. **17**, 1133 (1966).
[26]T. Jungwirth, J. Sinova, J. Mašek, J. Kučera, and A. H. MacDonald, Rev. Mod. Phys. **78**, 809 (2006).
[27]D. Natelson, R. L. Willett, K. W. West, and L. N. Pfeiffer, Appl. Phys. Lett. **77**, 1991 (2000).
[28]P. Granitzer, K. Rumpf, P. Pölt, A. Reichmann, M. Hofmayer, and H. Krenn, J. Magn. Magn. Mater. **316**, 302 (2007).
[29]S. Blundell, *Magnetism in Condensed Matter* (Oxford University Press, Oxford, 2009).
[30]R. A. de Groot, F. M. Mueller, P. G. van Engen, and K. H. J. Buschow, Phys. Rev. Lett. **50**, 2024 (1983).
[31]G. Tatara and H. Fukuyama, Phys. Rev. Lett. **78**, 3773 (1997).
[32]V. Korenman, J. L. Murray, and R. E. Prange, Phys. Rev. B **16**, 4032 (1977).
[33]B. Braunecker, P. Simon, and D. Loss, Phys. Rev. Lett. **102**, 116403 (2009).
[34]B. Braunecker, P. Simon, and D. Loss, Phys. Rev. B **80**, 165119 (2009).
[35]J. W. Negele and H. Orland, *Quantum Many-Particle Systems* (Westview Press, Boulder, CO, 1998).
[36]R. G. Pereira, master's thesis, Universidade Estadual de Campinas Instituto de Fisica Gleb Wataghin, 2004.
[37]M. Fabrizio and A. O. Gogolin, Phys. Rev. B **51**, 17827 (1995).
[38]P. Chudzinski, M. Gabay, and T. Giamarchi, Phys. Rev. B **81**, 165402 (2010).
[39]L. Balents and M. P. A. Fisher, Phys. Rev. B **53**, 12133 (1996).
[40]S. Eggert and S. Rommer, Phys. Rev. Lett. **81**, 1690 (1998).
[41]F. Anfuso and S. Eggert, Phys. Rev. Lett. **96**, 017204 (2006).
[42]S. Eggert, O. F. Syljuasen, F. Anfuso, and M. Andres, Phys. Rev. Lett. **99**, 097204 (2007).
[43]J. Sirker and N. Laflorencie, Europhys. Lett. **86**, 57004 (2009).
[44]R. G. Pereira, J. Sirker, J.-S. Caux, R. Hagemans, J. M. Maillet, S. R. White, and I. Affleck, J. Stat. Mech.: Theory Exp. (2007) P08022.
[45]T. Taniguchi, J. Sato, and H. Imamura, Phys. Rev. B **79**, 212410 (2009).
[46]E. M. Lifschitz and L. P. Pitaevskii, *Statistical Physics Part 2: Theory of the Condensed State* (Butterworth-Heinemann, London, 2002).
[47]T. Gilbert, IEEE Trans. Magn. **40**, 3443 (2004).
[48]S. Zhang and Z. Li, Phys. Rev. Lett. **93**, 127204 (2004).